

## Isoindolinone Inhibitors of the Murine Double Minute 2 (MDM2)-p53 Protein–Protein Interaction: Structure–Activity Studies Leading to Improved Potency

Ian R. Hardcastle,<sup>\*,†</sup> Junfeng Liu,<sup>‡</sup> Eric Valeur,<sup>†</sup> Anna Watson,<sup>†</sup> Shafiq U. Ahmed,<sup>‡</sup> Timothy J. Blackburn,<sup>†</sup> Karim Bennaceur,<sup>‡</sup> William Clegg,<sup>†</sup> Catherine Drummond,<sup>‡</sup> Jane A. Endicott,<sup>§</sup> Bernard T. Golding,<sup>†</sup> Roger J. Griffin,<sup>†</sup> Jan Gruber,<sup>§</sup> Karen Haggerty,<sup>†</sup> Ross W. Harrington,<sup>†</sup> Claire Hutton,<sup>‡</sup> Stuart Kemp,<sup>†</sup> Xiaohong Lu,<sup>‡</sup> James M. McDonnell,<sup>§</sup> David R. Newell,<sup>‡</sup> Martin E. M. Noble,<sup>§</sup> Sara L. Payne,<sup>†</sup> Charlotte H. Revill,<sup>†</sup> Christiane Riedinger,<sup>§</sup> Qing Xu,<sup>‡</sup> and John Lunec<sup>\*,‡</sup>

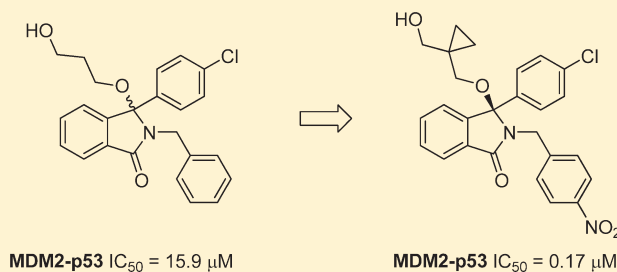
<sup>†</sup>Newcastle Cancer Centre, Northern Institute for Cancer Research and School of Chemistry, Bedson Building, Newcastle University, Newcastle, NE1 7RU, United Kingdom

<sup>‡</sup>Newcastle Cancer Centre, Northern Institute for Cancer Research, Paul O’Gorman Building, Medical School, Framlington Place, Newcastle University, Newcastle, NE2 4HH, United Kingdom

<sup>§</sup>Laboratory of Molecular Biophysics, Department of Biochemistry, University of Oxford, South Parks Road, Oxford, OX1 3QU, United Kingdom

**S** Supporting Information

**ABSTRACT:** Inhibition of the MDM2-p53 interaction has been shown to produce an antitumor effect, especially in MDM2 amplified tumors. The isoindolinone scaffold has proved to be versatile for the discovery of MDM2-p53 antagonists. Optimization of previously reported inhibitors, for example, NU8231 (7) and NU8165 (49), was guided by MDM2 NMR titrations, which indicated key areas of the binding interaction to be explored. Variation of the 2-*N*-benzyl and 3-alkoxy substituents resulted in the identification of 3-(4-chlorophenyl)-3-((1-(hydroxymethyl)cyclopropyl)methoxy)-2-(4-nitrobenzyl)isoindolin-1-one (74) as a potent MDM2-p53 inhibitor ( $IC_{50} = 0.23 \pm 0.01 \mu M$ ). Resolution of the enantiomers of 74 showed that potent MDM2-p53 activity primarily resided with the (+)-*R*-enantiomer (74a;  $IC_{50} = 0.17 \pm 0.02 \mu M$ ). The cellular activity of key compounds has been examined in cell lines with defined p53 and MDM2 status. Compound 74a activates p53, MDM2, and p21 transcription in MDM2 amplified cells and shows moderate selectivity for wild-type p53 cell lines in growth inhibition assays.



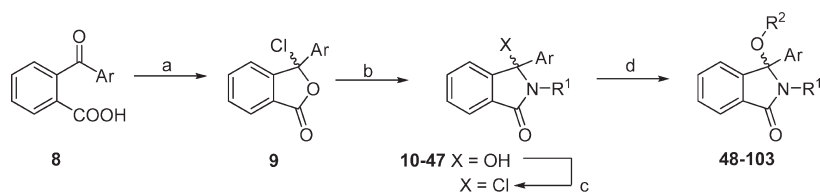
## INTRODUCTION

The response of the tumor suppressor protein p53 to cellular stresses, such as hypoxia, DNA damage, and oncogenic activation, is to act as a signaling node in the diverse pathways that become activated. Phosphorylation of p53, resulting from activation of kinases including ATM, CHK1 and 2, and DNA-PK, results in a stabilized and transcriptionally active form of the protein.<sup>1</sup> The resulting transcription of a range of genes is responsible for diverse functions, such as apoptosis, survival, cell-cycle arrest, DNA repair, angiogenesis, invasion, and auto-regulation, giving rise to the observed cellular effect.<sup>1,2</sup> The eventual fate of a cell, that is, apoptosis, cell-cycle arrest, or senescence, following p53 activation is thought to be determined by its genetic background. For tumor cells, the apoptotic pathway may be favored due to the loss of tumor suppressor proteins and associated cell cycle checkpoint controls, coupled with oncogenic stress.<sup>3</sup>

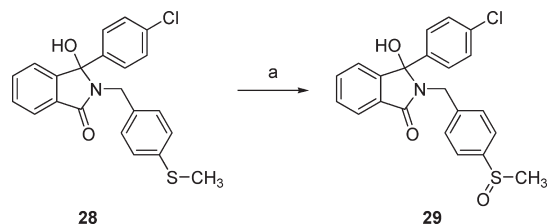
Inactivation of p53 by a range of mechanisms is a frequent causal event in the development and progression of cancer. These include inactivation by mutation, targeting by oncogenic viruses, and, in a significant proportion of cases, amplification of the MDM2 gene, resulting in overexpression or increased activation of the MDM2 protein. MDM2 amplification has been reported to occur in approximately 11% of all tumors and is found at higher levels in certain tumor types, for example, hepatocellular carcinoma (44%), osteosarcomas (20%), and soft tissue sarcomas (31%).<sup>4,5</sup> Normally, transcriptional activation of MDM2 by activated p53 results in increased MDM2 protein levels, forming a negative feedback loop.<sup>6,7</sup> MDM2 binds to the p53 transactivation domain, blocking p53-dependent transcriptional activity. MDM2 also functions as an E3 ligase, which

Received: September 13, 2010

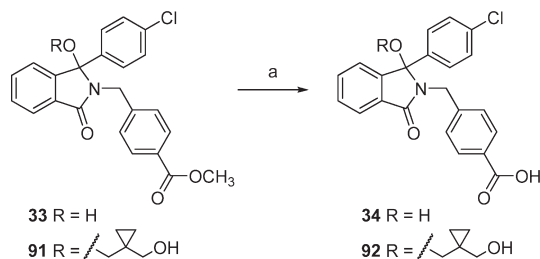
Published: February 11, 2011

Scheme 1. Synthesis of Substituted Isoindolinones 48–103<sup>a</sup>

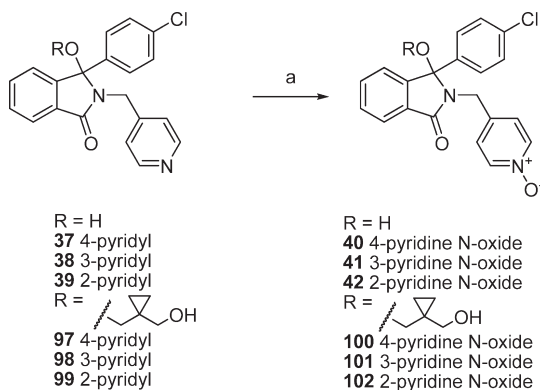
<sup>a</sup> Reagents and conditions: (a) SOCl<sub>2</sub>, DMF, THF; (b) R<sup>1</sup>NH<sub>2</sub>, *i*-Pr<sub>2</sub>EtN, or Et<sub>3</sub>N, THF; (c) SOCl<sub>2</sub>, DMF, THF; (d) R<sup>2</sup>OH, K<sub>2</sub>CO<sub>3</sub>, or *i*-Pr<sub>2</sub>EtN, THF.

Scheme 2. Synthesis of Sulfoxide 29<sup>a</sup>

<sup>a</sup> Reagents and conditions: (a) mCPBA, DCM.

Scheme 3. Synthesis of Benzoic Acids 34 and 91<sup>a</sup>

<sup>a</sup> Reagents and conditions: (a) (CH<sub>3</sub>)<sub>3</sub>SiOK, THF.

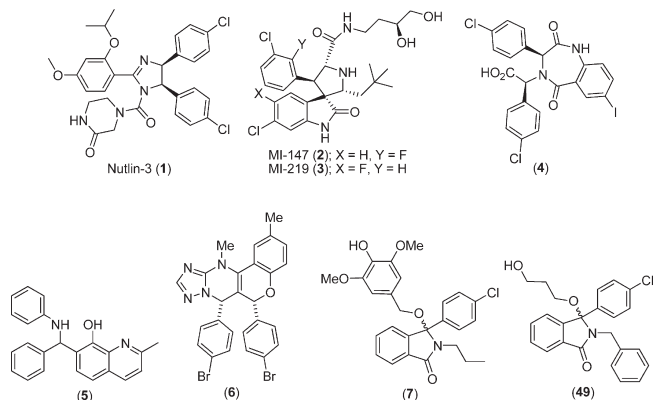
Scheme 4. Synthesis of Pyridine N-Oxides 40–42 and 100–102<sup>a</sup>

<sup>a</sup> Reagents and conditions: (a) mCPBA, DCM.

ubiquitylates the MDM2-p53 complex and has been shown to export the complex from the nucleus and target it for proteasomal destruction.<sup>8,9</sup>

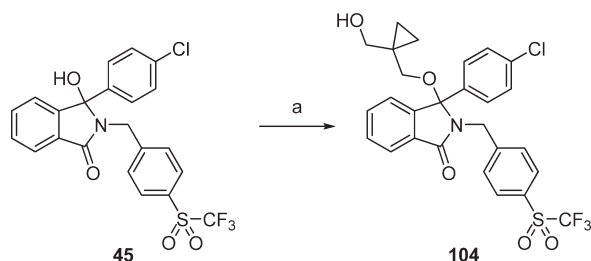
The tractability of the MDM2-p53 interaction as a drug target has been demonstrated and a number of classes of potent inhibitors

have been reported.<sup>10–12</sup> The most widely studied series to date are the Nutlins, for example, Nutlin-3 (**1**),<sup>13</sup> and the spirooxindoles, for example, MI-147 and MI-219 (**2**, **3**);<sup>14,15</sup> both series have demonstrated cellular activity consistent with MDM2-p53 inhibition and have shown *in vivo* antitumor activity.<sup>13,16</sup> Other small-molecule inhibitors include benzodiazepinediones (**4**),<sup>17,18</sup> 2-methyl-7-(phenyl(phenylamino)methyl)quinolin-8-ol (**5**),<sup>19</sup> and chromenotriazolopyrimidines (**6**).<sup>20</sup> Previously, we have reported isoindolinones, for example, NU8231 (**6**) and NU8165 (**49**) with low micromolar MDM2-p53 inhibitory potency and cellular activity.<sup>21</sup> In this paper, we describe the application of NMR-based structural biology and SAR studies to inform binding models, leading to MDM2-p53 inhibitory isoindolinones with significantly improved potency and cellular activity over the parent compounds.

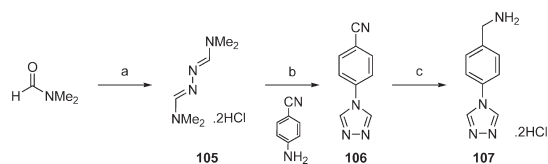


## CHEMISTRY

Substituted isoindolinones were prepared using the method described previously.<sup>21,22</sup> The appropriate benzoylbenzoic acids (**8a–d**) were converted into the corresponding  $\psi$ -acid chlorides (**9a–d**), which were condensed with the R<sup>1</sup>-primary amines to give the 4-hydroxyisoindolinones (**10–47**). The 4-hydroxy compounds (**10–47**) were converted into their respective chlorides and subsequently reacted with the appropriate alcohol in the presence of base (Et<sub>3</sub>N or DIPEA) to give the final substituted isoindolinones (**48–104**) as racemates (Scheme 1). The 4-methylsulfoxide (**29**) was prepared from the 4-methylthio derivative (**28**) by oxidation with mCPBA (Scheme 2). The 4-carboxylic acids (**34** and **92**) were prepared by cleavage of the corresponding methyl esters (**34** and **91**) by saponification with potassium trimethylsilylanolate in THF (Scheme 3). The 2-, 3-, and 4-pyridine N-oxides (**40–42** and **100–102**) were prepared by the reaction of the parent pyridines with mCPBA in DCM (Scheme 4). The 4-trifluoromethylsulfone derivative (**104**) was prepared from the 3-hydroxy precursor (**45**) directly using boron trifluoride etherate to activate the 3-hydroxyl group, followed by reaction with the

Scheme 5. Synthesis of Trifluoromethylsulfone **104**<sup>a</sup>

<sup>a</sup> Reagents and conditions: (a) (i)  $\text{BF}_3 \cdot \text{Et}_2\text{O}$ , DCM, 0 °C; (ii) 1,1-bis(hydroxymethyl)cyclopropane, DCM, 0 °C.

Scheme 6. Synthesis of 4-(4-(Ammoniomethyl)phenyl)-4*H*-1,2,4-triazol-4-ium Chloride **107**<sup>a</sup>

<sup>a</sup> Reagents and conditions: (a) (i)  $\text{SOCl}_2$ , 5 °C to r.t.; (ii)  $\text{NH}_2\text{NH}_2 \cdot \text{H}_2\text{O}$ , r.t.; (b) toluene, reflux; (c)  $\text{H}_2$ , 10% Pd/C, MeOH, aq. HCl.

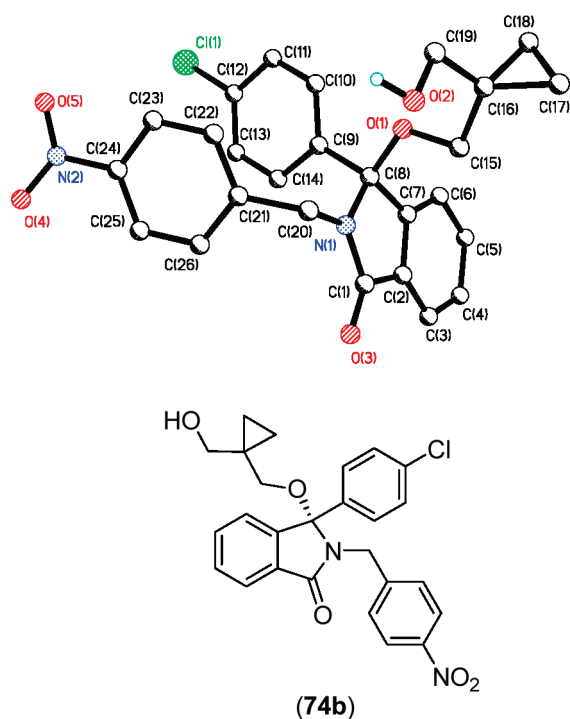
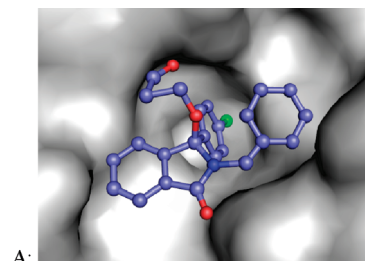


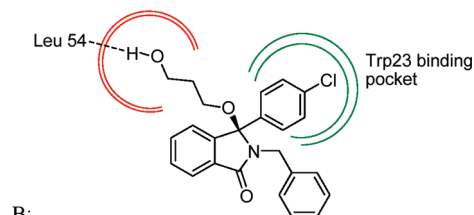
**Figure 1.** X-ray structure of **74b**, indicating the (*S*)-enantiomer.

relevant diol (Scheme 5). The 4-(1,2,4-triazolyl)benzylamine precursor was prepared by the reaction of dimethylaminomethylene-*N,N*-dimethylformohydrazonamide (**105**)<sup>23</sup> and 4-aminobenzonitrile, followed by reduction of the nitrile (**106**) to the methylamine (**107**; Scheme 6).

Compound **74** was resolved by HPLC using a chiral column. The (–)-enantiomer **74b** was crystallized from EtOAc and



A:



B:

**Figure 2.** Structure of (*R*)-NU8165 bound to MDM2 deduced from <sup>15</sup>N–<sup>13</sup>C HSQC NMR studies: (A) GOLD docked structure; (B) binding mode cartoon.

petrol by vapor diffusion, enabling a high-resolution X-ray crystal structure to be obtained that established the absolute stereochemistry as (*S*) (Figure 1). Suitable crystals were not obtained for the (+)-enantiomer **74a**.

## RESULTS AND DISCUSSION

**Structure-Based Design.** In our previous studies, we demonstrated the limitations of computer docking approaches in guiding the design of novel isoindolinone ligands for the p53-binding site of MDM2.<sup>21</sup> These studies were hampered by the large number of low energy binding modes available. As a result, we sought to gain structural information with key inhibitors bound to MDM2 through X-ray crystallography and NMR experiments. Unfortunately, to date, suitable cocrystals of isoindolinones bound to MDM2 have not been obtained. By contrast, NMR has provided useful structural information, despite the relatively low affinities of the ligands employed.<sup>24</sup> Initial NMR experiments using **6** ( $\text{IC}_{50} = 16 \mu\text{M}$ ) showed a significant chemical shift change in the Leu54 region attributed to an interaction with the hydroxypropoxy substituent (Figure 2). Reasoning that additional potency may be gained by introducing rigidity to the 3-alkoxy substituent, the *cis*-cyclopentyl derivative **50a** was proposed (Figure 3). The binding mode model for **6** also suggested that the substitution of the *N*-benzyl moiety could introduce additional favorable interactions and, hence, improve potency.

**Structure–Activity Relationships for Inhibition of the MDM2–p53 Interaction. 3-Hydroxy Isoindolinones.** To understand the relative contributions to potency of the substituents on the isoindolinone scaffold, the 3-hydroxyisoindolinones were assayed for their MDM2–p53 inhibitory activity (Table 1). The introduction of small, lipophilic substituents at the 4-position of the *N*-benzyl group resulted in significant gains in potency, for example, the 4-chloro compound (**13**) is 17 times more potent than the parent compound (**11**). Similarly, the introduction of a 4-nitro substituent (**20**) resulted in a 30-fold improvement in potency over **11**. Retaining the 4-nitrobenzyl substituent and varying the 3-aryl substituent demonstrated that the 4-chloro or 4-bromo substituents confer the greatest potency (**20** and **21**)

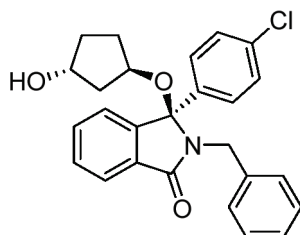
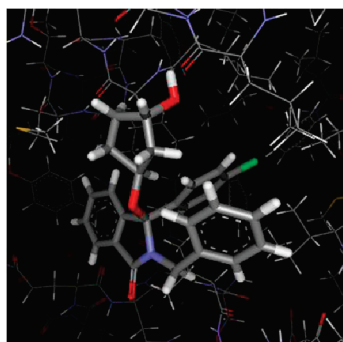


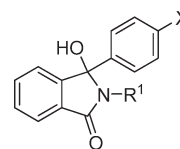
**Figure 3.** Modeled structure of the *trans*-(*R*)-3-((1*R*,3*R*)-3-hydroxycyclopentyl)oxy analogue of NU8165.

compared with the unsubstituted 3-phenyl (**18**), whereas the 4-fluoro compound (**19**) was less active. Switching the nitro group to the 3-position (**22**) resulted in a dramatic loss of activity. The 1-naphthyl (**26**) and 3-bromo (**27**) derivatives were similarly nonpotent, indicating a lack of tolerance for steric bulk at this position. Homologation of **11** to the phenethyl derivative (**23**) resulted in a 10-fold gain in potency, whereas, the 4-nitro- and 4-anilino-substituted phenethyl derivatives (**25** and **26**) did not gain additional potency. A range of additional 4-substituents was investigated, including classical and nonclassical isosteres of the nitro group (**29**–**42**). Of these, only the methyl 4-benzoate (**33**) retained significant activity.

**3-Alkoxy Isoindolinones.** A series of 3-alkoxyisoindolinones was assayed for MDM2-p53 inhibitory activity (Table 2). As predicted by the NMR-based binding model, the 3-hydroxycyclopentyl derivative (**50**), a mixture of *cis*- and *trans*-isomers, showed a 5-fold improvement in potency compared with the acyclic derivative (**6**), demonstrating the positive effect of conformational restriction of the alkoxy side chain. Gratifyingly, inclusion of the 4-nitrobenzyl group, observed to be beneficial in the 3-OH series, had an additive effect on potency (**51**). However, refinement of the stereochemistry to the *cis*-derivative **52** produced only a modest improvement in potency over the *cis/trans* mixture. The desired *trans*-diol was not commercially available, and attempts to epimerize the *cis*-derivative **52** met with failure. In contrast to the 3-hydroxy series, inclusion of a 4-cyanobenzyl group (**53**) did not improve potency significantly over **50**. Further conformational restriction was introduced with the unsaturated *cis*-3-hydroxycyclopent-2-enyloxy group. Introduction of 4-chloro or 4-methyl substituents resulted in modest gains in potency (**55** and **56**), and the 4-nitro substituent gave a similar gain in potency (**57**), although this compound was 5-fold less potent than **52**. Interestingly, the acyclic unsaturated *Z*-4-hydroxybut-2-enyloxy derivative **58** was equipotent with the *trans*-cyclopentyl derivative **50**.

The synthesis of the *cis*-3-hydroxycyclopentylisoindolinones, predicted to be favored by the model, was complicated by the lack

**Table 1.** 3-Hydroxyisoindolinone SAR: Variation of the 2-*N*-Benzyl Substituent

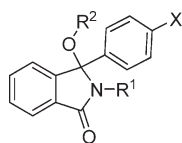


Compd	X	R <sup>1</sup>	IC <sub>50</sub> (μM)	Compd	X	R <sup>1</sup>	IC <sub>50</sub> (μM)
<b>10</b>	Cl	-CH <sub>2</sub> CH <sub>2</sub> CH <sub>3</sub>	69 ± 25	<b>27</b>	Cl		>100
<b>11</b>	Cl	-CH <sub>2</sub> Ph	74 ± 3	<b>28</b>	Cl		>20
<b>12</b>	Cl		>20	<b>29</b>	Cl		>100
<b>13</b>	Cl		4.2 ± 0.4	<b>30</b>	Cl		>100
<b>14</b>	Cl		4.5 ± 0.4	<b>31</b>	Cl		>100
<b>15</b>	Cl		>20	<b>32</b>	Cl		>100
<b>16</b>	Cl		15 ± 3	<b>33</b>	Cl		11 ± 4
<b>17</b>	Cl		6.0 ± 1.8	<b>34</b>	Cl		>100
<b>18</b>	H		87 <sup>a</sup>	<b>35</b>	Cl		88 <sup>a</sup>
<b>19</b>	F		9.5 <sup>a</sup>	<b>36</b>	Cl		>20
<b>20</b>	Cl		2.4 ± 0.2	<b>37</b>	Cl		>20
<b>21</b>	Br		3.1 ± 0.2	<b>38</b>	Cl		>200
<b>22</b>	Cl		54 ± 14	<b>39</b>	Cl		>200
<b>23</b>	Cl		7.2 ± 2.0	<b>40</b>	Cl		>200
<b>24</b>	Cl		6.2 ± 1.6	<b>41</b>	Cl		>200
<b>25</b>	Cl		6.2 ± 1.6	<b>42</b>	Cl		>200
<b>26</b>	Cl		47 <sup>a</sup>				

<sup>a</sup> *n* = 1.

of available starting materials, and efforts to epimerize final *trans*-compounds met with failure. As an alternative, the acyclic derivatives were revisited with the inclusion of selected favorable 4-substituted benzyl groups identified in the 3-OH series. Interestingly, in the 4-nitro series, the hydroxypropoxy and hydroxybutoxy compounds **59** and **60** were equipotent with the *trans*-cyclic derivative **52**. The 4-cyanohydroxybutoxy compound **61** also exhibited similar potency to the corresponding *trans*-cyclic derivative **53**. Some stereospecificity of inhibition was observed with the 4-chloro- $\alpha$ -methylbenzylamine derivatives, the (*R*)-isomer **62** was 2-fold more potent than the (*S*)-isomer **63**, although **62** was 2-fold less potent than the 4-nitro derivative **61**. Homologation to the 4-nitrophenethylamino derivative **64** resulted in a 7-fold loss in activity. The modest drop in activity on replacement of 4-chlorophenyl by 4-bromophenyl was also seen in the hydroxypropoxy and hydroxybutoxy compounds **65** and **66**.

The SAR around the 3-alkoxy substituent was explored further, retaining the 4-nitrobenzyl group as optimal (Table 3). A range of suitable diols was introduced to probe the spatial and steric requirements at this position, and all the compounds prepared inhibited the MDM2-p53 interaction with submicromolar potency. The *trans*-1,4-cyclohexanedimethanol derivative **68** was nearly 2-fold more active than 1,4-phenylenedimethanol derivative **67**, which was the least potent in the series. The 1,3-phenylenedimethanol derivative **69** displayed improved potency compared with **67**. The *trans*-1,4-cyclooctane diol, *trans*-1,4-cyclohexane diol,

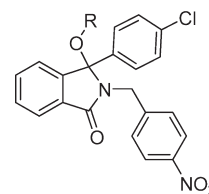
**Table 2. Isoindolinone SAR: Variation of the 2-*N*-Benzyl and 3-Alkoxy Substituent**

Compd	X	R <sup>1</sup>	R <sup>2</sup>	IC <sub>50</sub> (μM)
48	F	-CH <sub>2</sub> CH <sub>2</sub> CH <sub>3</sub>		>20
49	Cl	-CH <sub>2</sub> Ph	-(CH <sub>2</sub> ) <sub>3</sub> OH	16 ± 1*
50	Cl	-CH <sub>2</sub> Ph		3.0 ± 1.0
51	Cl			0.70 ± 0.16
52	Cl			0.40 ± 0.04
53	Cl			2.3 ± 0.3
54	Cl	-CH <sub>2</sub> Ph		4.7 ± 1.1
55	Cl			1.5 ± 0.3
56	Cl			1.4 ± 0.4
57	Cl			1.9 ± 0.3
58	Cl			0.40 ± 0.01
59	Cl		-(CH <sub>2</sub> ) <sub>3</sub> OH	0.45 ± 0.01
60	Cl		-(CH <sub>2</sub> ) <sub>4</sub> OH	0.36 ± 0.04
61	Cl		-(CH <sub>2</sub> ) <sub>4</sub> OH	3.5 ± 1.5
62	Cl		-(CH <sub>2</sub> ) <sub>4</sub> OH	0.9 ± 0.6
63	Cl		-(CH <sub>2</sub> ) <sub>4</sub> OH	2.5 ± 0.8
64	Cl		-(CH <sub>2</sub> ) <sub>4</sub> OH	3.2 ± 1.0
65	Br		-(CH <sub>2</sub> ) <sub>3</sub> OH	1.4 ± 1.6
66	Br		-(CH <sub>2</sub> ) <sub>4</sub> OH	0.57 ± 0.06

\* Ref 21.

and *trans*-1,4-cyclohex-2-ene diol derivatives **70**, **75**, and **76** showed similar activity to the 1,4-butanediol derivative **60**, whereas the but-2-yne-1,4-diol and the *cis*-1,2-cyclohexanedimethanol derivatives **71** and **72** were somewhat less potent. Steric restriction of the 1,3-propanediol chain with 2,2-dimethyl, 2-cyclopropyl, or 2-methylene groups (**73**, **74**, and **75**) maintained the potency of the parent **59**, with the 2-(1,1-cyclopropane)dimethanol derivative **74** showing the best activity in this series.

The possible pharmacological liabilities associated with the nitro group present in **74** prompted the evaluation of a number of alternatives including classical and nonclassical isosteres (Table 4). Replacement with simple lipophilic substituents (**78–86**) resulted in a 5–10-fold loss in potency, with the more potent being the cyano, bromo, and iodo derivatives (**78**, **81**, and **82**). The introduction of more sterically demanding, or *meta*-substituents, resulted in dramatic losses in potency, for example, trifluoromethyl (**89**) and the 1-naphthalene derivative (**87**). Isosteric and pseudoisosteric replacements for the nitro group were also inactive, for example, carboxyl (**92**), carboxamide (**94**), and acetyl (**95**). The 2-, 3- and 4-pyridyl isomers (**97–99**) lacked significant potency, as did their respective pyridine-*N*-oxides (**100–102**). We considered that the 1,2,4-triazolyl group could act as a nitro group bioisostere, as it has similar shape and electronic characteristics. Disappointingly, the 4-(1,2,4-triazolyl) derivative (**103**) was inactive, possibly indicating a lack of steric tolerance for the larger heterocycle. An aromatic nitro group was replaced successfully by a trifluoromethylsulfone group in the development of the Bcl-XL inhibitor ABT-737.<sup>25</sup> In our case, however, the same replacement (**104**) resulted in a complete loss of

**Table 3. 2-*N*-4-Nitrobenzylisoindolinone SAR: Variation of the 3-Alkoxy Substituent**

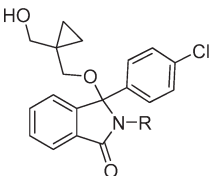
Compd	R	IC <sub>50</sub> (μM)
67		0.98 ± 0.02
68		0.58 ± 0.08
69		0.73 ± 0.13
70		0.38 ± 0.04
71		0.66 ± 0.11
72		0.57 ± 0.07
73		0.40 ± 0.08
74		0.23 ± 0.01
75		0.39 ± 0.11
76		0.31 ± 0.09

activity. These results suggest that the nitro group's interactions with the protein are mostly lipophilic and strongly directional and that its electron withdrawing character is also important.

The enantiomers of **74**, the most potent compound identified in this study, were separated by chiral HPLC and showed that potent MDM2-p53 activity resided with the (+)-*R*-enantiomer **74a** (IC<sub>50</sub> = 0.171 ± 0.015 μM). By contrast, the *S*-enantiomer **74b** was weakly active (IC<sub>50</sub> = 1.30 ± 0.11 μM). The binding mode for **74a** as deduced from NMR experiments and GOLD docking is similar to the original model for **6** (Figure 4).<sup>24</sup> The 2-(1,1-cyclopropane)dimethanol interacts with the surface of the region close to Leu54 of MDM2, a region not occupied by Nutlin-2 or the benzodiazepine **3**, as seen in X-ray structures (1rv1 and 1t4e). The 4-chlorophenyl group occupies the Ile99 pocket, also occupied by halophenyl groups in the Nutlin-2 and **3**. The deep pocket filled by Trp23 of p53 is occupied by the isoindolinone scaffold. The 4-nitrophenyl group occupies the Gln54 pocket, which is occupied by the piperidinone moiety of Nutlin-2 and the iodoaryl portion of **3**. The SAR for the 4-substituted phenyl group is not readily explained by this model and further structural studies are ongoing.

**Cell Biology.** Potent compounds identified in the cell-free ELISA were selected for investigation in intact cells. SJSA-1 cells (MDM2 amplified, p53wt) were treated with increasing concentrations of **68**, **70–74**, **74a**, and **74b** using Nutlin-3 as a positive control. Cells were lysed at a 6 h time point and protein

**Table 4.** 3-(1-Hydroxymethylcyclopropylmethoxy) isoindolinone SAR: Variation of the 2-N-Benzyl Substituent



Compd	R <sup>1</sup>	IC <sub>50</sub> (μM)	Compd	R <sup>1</sup>	IC <sub>50</sub> (μM)
78		1.8 ± 0.7	91		>20
79		2.6*	92		>20
80		2.3 ± 0.6	94		>50
81		1.2 ± 0.6	95		17*
82		1.5*	96		>100
83		2.3*	97		252*
84		2.8*	98		29 ± 6
85		8.8 ± 2.1	99		11 ± 1
86		8.9 ± 1.9	100		>200
87		49 (n = 2)	101		>200
88		47 (n = 2)	102		33 ± 3
89		214*	103		>20
90		175	104		>50

\* n = 1.

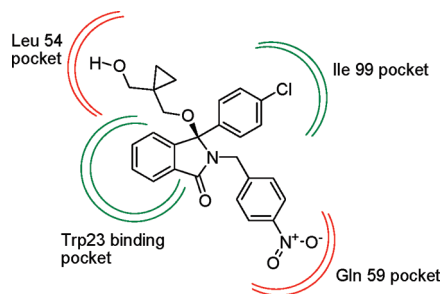


**Figure 4**

extracts analyzed by Western blotting, probing for MDM2, p53 and p21 to test for p53 pathway activation, and either actin or  $\alpha$ -tubulin as protein loading controls (Figures 5–7). Compounds 68, 70–74, 74a, and 74b produced a concentration-dependent induction of MDM2, p53, and p21 over the 1–20  $\mu$ M dose range, with 72, 68, and 74 showing greater induction of p53 and p21 at the 10  $\mu$ M point. Nutlin-3 showed comparable effects over a 1–10  $\mu$ M dose range. The enantiomers of 74, 74a, and 74b, and Nutlin-3 were compared over a 1–20  $\mu$ M dose range (Figure 7). The potent enantiomer 74a showed strong induction of MDM2, p53, and p21, whereas the less potent enantiomer 74b showed only weak activity at the highest concentration (20  $\mu$ M). The lack of cellular activity of 74b offers strong evidence that the cellular activation of p53 transcription by the isoindolinone inhibitors is mediated by their inhibition of MDM2-p53 binding.

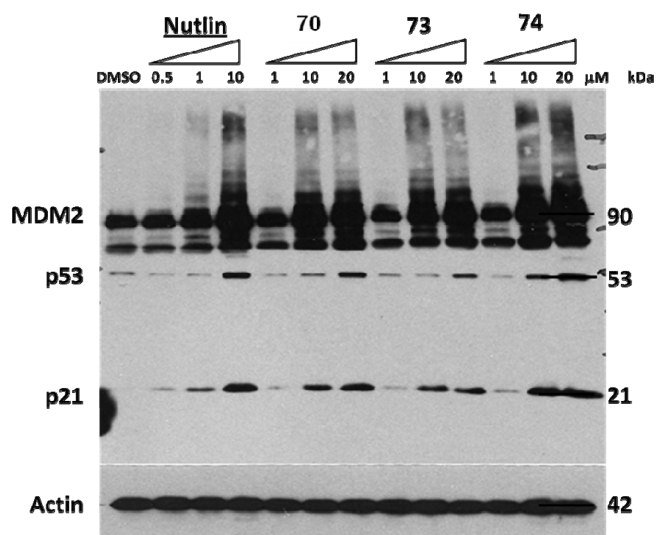


**Figure 5.** Cellular activity of 70, 73, and 74 for the p53 pathway activation detected by Western blotting (SJS-A1 cells, 4 h treatment).

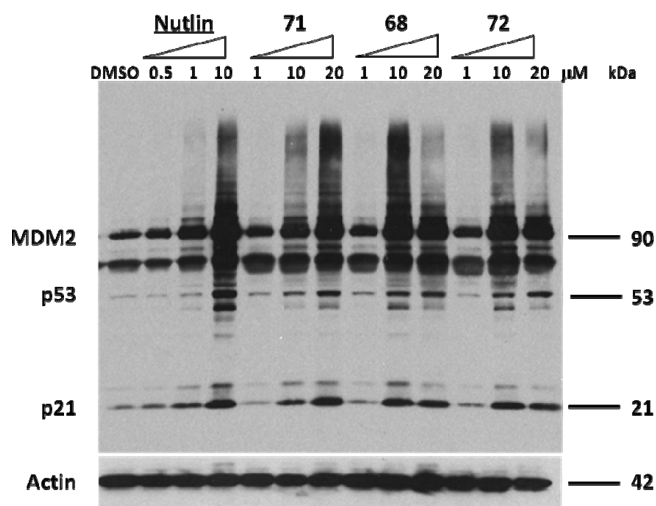


**Figure 6.** Cellular activity of 71, 68, and 72 for the p53 pathway activation detected by Western blotting (SJS-A1 cells, 4 h treatment).

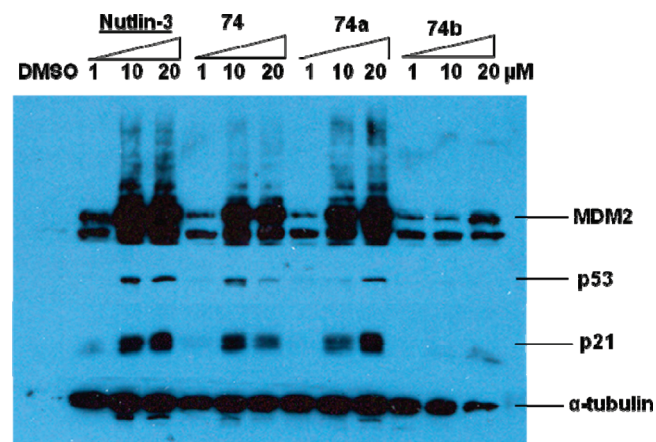


**Figure 7.** Cellular activity of 74, 74a, and 74b for the p53 pathway activation detected by Western blotting (SJS-A1 cells, 4 h treatment).

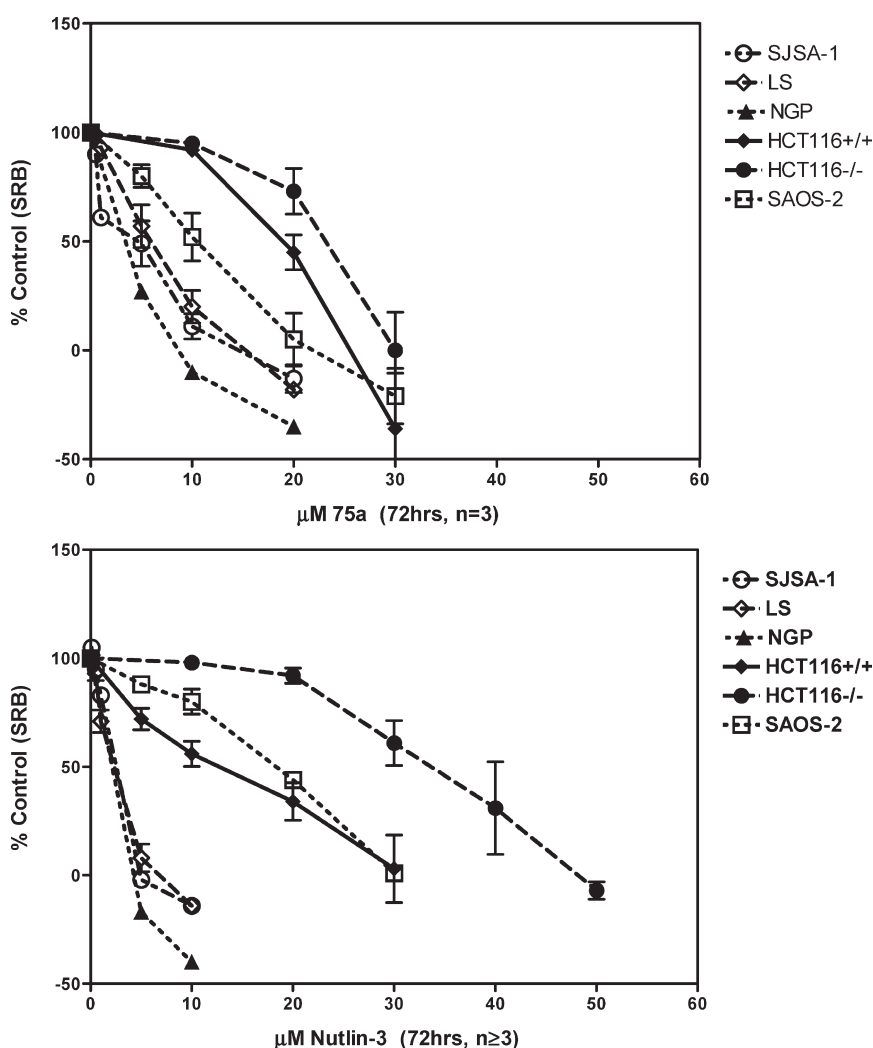


**Figure 8.** Comparison of concentration dependent growth inhibition of 74a and Nutlin-3 using an SRB-based growth inhibition assay in a panel of cell lines with differing MDM2 and p53 status.

**Table 5.** Growth Inhibitory Activity of 74 and Enantiomers in Comparison to Nutlin-3, as Determined by SRB Assay

compound	MDM2-p53 IC <sub>50</sub> (μM)	SJSA-1	SRB GI <sub>50</sub> <sup>a</sup> (μM)				
			LS	NGP <sup>b</sup>	HCT116(+/+)	HCT116(-/-)	SAOS
74	0.23 ± 0.01	8.3 ± 1.1 (n = 4)	6.9 ± 1.3 (n = 4)	6.9	15 ± 0.3	20 ± 1	8.9 ± 2.1
74a	0.17 ± 0.02	5.2 ± 1.5	6.1 ± 1.8	3.4	20 ± 2	24 ± 2	11 ± 3
74b	1.30 ± 0.11	20 ± 3	153 ± 4	13	21 ± 1	24 ± 1	14 ± 1
Nutlin-3	0.061 ± 0.021	2.6 ± 0.1	2.3 ± 0.3	2.1	13 ± 3	34 ± 4	18 ± 0.2

<sup>a</sup> Values are n = 3 unless otherwise stated. <sup>b</sup> n = 1.

The growth-inhibitory and cytotoxic effects of 74a and Nutlin-3 were compared in a range of cell lines using the SRB assay (Figure 8). Three MDM2 amplified cell lines were used, all wild type for p53 (SJSA-1 osteosarcoma, NGP and LS neuroblastoma), and three MDM2 nonamplified cell lines, an isogenic pair of wild type p53 and null colorectal cancer cell lines (HCT116 p53(+/-) and p53(-/-) colon), and a p53 null osteosarcoma cell line (SaOS-2). The results for both compounds show that MDM2 amplified cell lines were more sensitive to the growth inhibitory effects of MDM2-p53 inhibition. A comparison of GI<sub>50</sub> values showed that 74a was 2–3-fold

less growth inhibitory than Nutlin-3 in the three MDM2-amplified cell lines consistent with the 2.5-fold lower potency versus MDM2-p53 of 74a (Table 5). The less-active enantiomer 74b was 6–10-fold less growth inhibitory than Nutlin-3 but is approximately 20-fold less potent versus MDM2-p53, suggesting that some nonspecific growth inhibitory activity is present. Nutlin-3 showed the greatest difference in activity in the paired p53(+/-) and (-/-) HCT-116 cell lines and had the lowest potency in the p53 null SAOS line. These results suggest that the initial growth inhibitory activity of the MDM2-p53 inhibitors tested resulted from MDM2-mediated p53 activation but that, at

higher concentrations, non-p53 related off-target effects resulted in additional growth inhibitory activity.

## CONCLUSIONS

The isoindolinone series of MDM2-p53 inhibitors has been optimized for potency and cellular activity. The addition of a 4-nitro substituent to the *N*-benzyl moiety of **6** resulted in a greater than 30-fold improvement in potency (**59**,  $IC_{50} = 0.45 \pm 0.01 \mu\text{M}$ ). A further gain was achieved by introducing conformational restriction to the isoindolinone 3-hydroxypropoxy side-chain in the form of a 2-cyclopropyl group (**74**,  $IC_{50} = 0.23 \pm 0.01 \mu\text{M}$ ). As expected, only one enantiomer (*R*)-**74a** ( $IC_{50} = 0.17 \pm 0.02 \mu\text{M}$ ) was responsible for the inhibitory potency of the racemate. The cellular activation of p53 of **74a** was similar to Nutlin-3, albeit at a lower potency. Similarly, the profile of growth inhibitory activity in cell lines with defined p53 and MDM2 status was similar to Nutlin-3, however, p53-independent, off-target effects were seen at lower concentrations than for Nutlin-3. We consider that the isoindolinones such as **74a** are promising leads for the development of MDM2-p53 targeted cancer therapeutics. Further studies are ongoing to address the potency, selectivity, and drug-like properties for this class of inhibitors.

## EXPERIMENTAL SECTION

**General Methods.** Reagents were purchased from fine chemicals vendors, and used as received unless otherwise stated. Solvents were purified and stored according to standard procedures. Petrol refers to that fraction in the boiling range 40–60 °C. THF refers to anhydrous tetrahydrofuran, either by distillation from sodium benzophenone, or from commercial sources. Melting points were obtained on a Stuart Scientific SMP3 apparatus and are uncorrected. Thin layer chromatography was performed using silica gel plates (Kieselgel 60F<sub>254</sub>; 0.2 mm), and visualized with UV light or potassium permanganate. Chromatography was conducted under medium pressure in glass columns or using a Biotage SP4 instrument in prepacked columns (FLASH+ Silica columns (40–63  $\mu\text{m}$ , 60 Å)). Chiral semipreparative HPLC was conducted using a Varian Prostar instrument equipped with a Daicel Chiralpak AD-H 250  $\times$  10 mm column eluting with hexane, ethanol (4:1), at a flow rate of 3.5 mL/min, monitoring by UV at  $\lambda = 270 \text{ nm}$ . Proton (<sup>1</sup>H) and carbon (<sup>13</sup>C) nuclear magnetic resonance (NMR) spectra were recorded on a Bruker Spectrospin AC 300E (<sup>1</sup>H at 300 MHz, <sup>13</sup>C at 75 MHz), a Jeol JNM-LA500 spectrometer (<sup>1</sup>H at 500 MHz, <sup>13</sup>C at 125 MHz), or a Bruker Avance II 500 (<sup>1</sup>H at 500 MHz, <sup>13</sup>C at 125 MHz) employing the solvent as internal standard. IR spectra were recorded on a Bio-Rad FTS 3000MX diamond ATR. Liquid chromatography–mass spectrometry (LCMS) was carried out on a Micromass Platform instrument operating in positive and negative ion electrospray mode, employing a 50  $\times$  4.6 mm C18 column (Waters Symmetry or Waters Atlantis) 5 or 12 min gradient elution with 0.05% formic acid in methanol (10–90%). All compounds gave  $\geq 95\%$  purity by <sup>1</sup>H NMR, HPLC, or LCMS, unless stated otherwise. Elemental analyses were performed by The School of Pharmacy, Analytical Facility, University of London, WC1N 1AX. Accurate masses were measured using a Finnigan MAR 95 XP or a Finnigan MAR 900 XLT at the EPSRC National Mass Spectrometry Service Centre (Chemistry Department, University of Wales, Swansea, Wales, SA2 8PP).

**General Procedure A: 3-Hydroxy Compounds.** To a solution of the appropriate benzoic acid (1 equiv) in THF (10 mL), under N<sub>2</sub>, was added thionyl chloride (2 equiv) and 3 drops of anhydrous DMF, and the resulting mixture was stirred for 4 h at rt and then concentrated in vacuo. The residue was diluted with THF (10 mL), and

the required amine (1.1 equiv) and DIPEA (1.1 equiv) or Et<sub>3</sub>N (1.1 equiv) were added, under N<sub>2</sub>. The resulting mixture was stirred overnight at rt and then concentrated in vacuo. The residue was diluted with EtOAc (50 mL) and filtered, and the filtrate washed with water (3  $\times$  25 mL) and brine (1  $\times$  25 mL). The organic layer was dried (MgSO<sub>4</sub> or Na<sub>2</sub>SO<sub>4</sub>) and concentrated in vacuo to afford the required 3-hydroxyisoindolinone as a solid, which was recrystallized (EtOAc, petrol) or purified by chromatography.

**General Procedure B: 3-Alkoxy Isoindolinones.** To a solution of the appropriate isoindolinone (1.37 mmol, 1 equiv) in THF (10 mL) under N<sub>2</sub> was added thionyl chloride (2 equiv) and 3 drops of DMF, and the resulting mixture was stirred for 4 h at rt and then concentrated in vacuo. The residue was diluted with THF (10 mL) and the required alcohol (2 equiv), potassium carbonate (2 equiv) or DIPEA (1.1 equiv) were added, and the resulting mixture was stirred overnight at rt and then concentrated in vacuo. The residue was diluted with EtOAc (50 mL) and washed with water (3  $\times$  25 mL) and brine (1  $\times$  25 mL). The organic layer was dried (MgSO<sub>4</sub>) and concentrated in vacuo to afford an oil that was purified by chromatography (silica; EtOAc/petrol).

**E-3-(4-Chlorophenyl)-3-(4-hydroxybut-2-enyloxy)-2-(4-nitrobenzyl)-2,3-dihydroisoindol-1-one (58).** General Procedure B: **20** (400 mg, 1.0 mmol), thionyl chloride (214  $\mu\text{L}$ , 2.75 mmol), *cis*-butenediol (445 mg, 5.0 mmol), and K<sub>2</sub>CO<sub>3</sub> (380 mg, 2.75 mmol) gave **58** as a yellow oil (272 mg, 58%): <sup>1</sup>H NMR (300 MHz, CDCl<sub>3</sub>)  $\delta$  1.70 (br s, 1H, OH), 3.32 (dd, 1H,  $J = 12.1, 6.3 \text{ Hz}$ , OCH), 3.45 (dd, 1H,  $J = 12.1, 6.3 \text{ Hz}$ , OCH'), 3.79 (d, 2H,  $J = 6.6 \text{ Hz}$ , HOCH<sub>2</sub>), 4.25 (d, 1H,  $J = 15.0 \text{ Hz}$ , N–CH), 4.64 (d, 1H,  $J = 15.0 \text{ Hz}$ , N–CH'), 5.26–5.35 (m, 1H, OCH<sub>2</sub>CH), 5.53–5.62 (m, 1H, OCH<sub>2</sub>CH'), 7.12–7.23 (m, 5H, Ar–H), 7.36–7.39 (m, 2H, Ar–H), 7.51–7.57 (m, 2H, Ar–H), 7.91–7.93 (m, 1H, C(O)=C=CH), 8.00–8.04 (m, 2H, Ar–H); <sup>13</sup>C NMR (75 MHz, CDCl<sub>3</sub>)  $\delta$  42.57, 58.48, 59.20, 95.0, 123.4, 123.9, 126.8, 128.0, 128.7, 130.0, 130.2, 131.4, 132.0, 133.1, 135.0, 136.9, 144.6, 145.1, 147.5, 168.2; (ESI+)  $m/z = 465 [M + H]^+$ ; CHN.

**3-(4-Chlorophenyl)-3-(3-hydroxypropoxy)-2-(4-nitrobenzyl)-2,3-dihydroisoindol-1-one (59).** General Procedure B: **20** (400 mg, 1.0 mmol), 1,3-propanediol (365  $\mu\text{L}$ , 5.1 mmol), thionyl chloride (214  $\mu\text{L}$ , 2.75 mmol), and potassium carbonate (380 mg, 2.75 mmol). Chromatography (silica; 40% EtOAc, petrol) gave **59** as a yellow solid (342 mg, 75%): mp 141–143 °C; IR (cm<sup>-1</sup>) 3397, 1682 cm<sup>-1</sup>; <sup>1</sup>H NMR (300 MHz, CDCl<sub>3</sub>)  $\delta$  1.49–1.60 (m, 2H, OCH<sub>2</sub>CH<sub>2</sub>), 1.65 (br s, 1H, OH), 2.94 (m, 2H, OCH<sub>2</sub>), 3.62 (t, 2H,  $J = 6.0 \text{ Hz}$ , HOCH<sub>2</sub>), 4.33 (d, 1H,  $J = 15.0 \text{ Hz}$ , N–CH), 4.63 (d, 1H,  $J = 15.0 \text{ Hz}$ , N–CH'), 7.14–7.20 (m, 5H, Ar–H), 7.36–7.40 (m, 2H, Ar–H), 7.52–7.58 (m, 2H, Ar–H), 7.92–7.94 (m, 1H, C(O)=C=CH), 8.02–8.06 (m, 2H, Ar–H); <sup>13</sup>C NMR (75 MHz, CDCl<sub>3</sub>)  $\delta$  32.1, 42.4, 60.0, 60.5, 94.9, 123.1, 123.3, 123.9, 127.9, 128.7, 129.9, 130.1, 131.5, 133.0, 134.9, 137.1, 144.7, 145.2, 147.4, 168.2; LCMS (ESI+)  $m/z$  453  $[M + H]^+$ . CHN.

**3-(4-Chlorophenyl)-3-(4-hydroxybutoxy)-2-(4-nitrobenzyl)-2,3-dihydroisoindol-1-one (60).** General Procedure B: **20** (400 mg, 1.0 mmol), 1,4-butanediol (455 mg, 5.0 mmol), thionyl chloride (214  $\mu\text{L}$ , 2.75 mmol), and potassium carbonate (380 mg, 2.75 mmol). Chromatography (silica; 40% EtOAc, petrol) gave **60** as a yellow oily solid (320 mg, 68%). IR (cm<sup>-1</sup>) 3440, 2940, 1697, 1519; <sup>1</sup>H NMR (300 MHz, CDCl<sub>3</sub>)  $\delta$  1.21–1.51 (m, 4H, OCH<sub>2</sub>CH<sub>2</sub>CH<sub>2</sub>), 1.62 (br s, 1H, OH), 2.77 (t, 2H,  $J = 5.1 \text{ Hz}$ , OCH<sub>2</sub>), 3.52 (t, 2H,  $J = 5.7 \text{ Hz}$ , HOCH<sub>2</sub>), 4.25 (d, 1H,  $J = 15.0 \text{ Hz}$ , N–CH), 4.62 (d, 1H,  $J = 15.0 \text{ Hz}$ , N–CH'), 7.08–7.22 (m, 5H, Ar–H), 7.39–7.35 (m, 2H, Ar–H), 7.49–7.55 (m, 2H, Ar–H), 7.88–7.94 (m, 1H, C(O)=C=CH), 8.04–8.01 (m, 2H, Ar–H); <sup>13</sup>C NMR (75 MHz, CDCl<sub>3</sub>)  $\delta$  25.7, 29.4, 42.4, 62.3, 62.9, 94.8, 123.1, 123.3, 123.8, 128.0, 128.7, 130.0, 130.0, 131.4, 133.0, 134.8, 137.2, 144.8, 145.3, 147.4, 168.2; (ES)  $m/z$ :  $[M]^+$ . CHN.

**3-(4-Bromophenyl)-3-(4-hydroxybutoxy)-2-(4-nitrobenzyl) isoindolin-1-one (66).** General Procedure B: **21** (0.50 g, 1.1 mmol), thionyl chloride (214  $\mu\text{L}$ , 2.75 mmol), 1,4-butanediol (0.20 mL, 2.3

mmol), and  $K_2CO_3$  (526 mg, 5.0 mmol). Chromatography (Biotage SP4, silica; 10–50% EtOAc, petrol) gave **66** as a pale yellow oil (0.50 g, 85%). IR ( $cm^{-1}$ ) 3397, 2925, 2872, 1687, 1605, 1519, 1467;  $^1H$  NMR (300 MHz,  $CDCl_3$ )  $\delta$  1.36–1.45 (m, 4H,  $(CH_2)_2$ ), 2.76 (t, 1H,  $J = 6.1$  Hz,  $OCH_2$ ), 3.49 (t, 2H,  $J = 6.2$  Hz,  $HOCH_2$ ), 4.25 (d, 1H,  $J = 15.0$  Hz,  $N-CH$ ), 4.60 (d, 1H,  $J = 15.0$  Hz,  $N-CH'$ ), 7.08–7.13 (m, 3 H, Ar–H), 7.29–7.36 (m, 4H, Ar–H), 7.48–7.51 (m, 2H, Ar–H), 7.87–7.89 (m, 1H,  $C(O)=C=CH$ ), 7.97–8.00 (m, 2H, Ar–H);  $^{13}C$  NMR (75 MHz,  $CDCl_3$ )  $\delta$  26.0, 29.7, 42.7, 62.5, 63.2, 95.1, 123.2, 123.5, 123.6, 124.1, 128.6, 130.3, 130.3, 131.8, 131.9, 133.3, 138.1, 145.1, 145.6, 147.7, 168.5; CHN.

**3-(4-Chlorophenyl)-3-(5-hydroxycyclooctyloxy)-2-(4-nitrobenzyl)-2,3-dihydroisoindol-1-one (70)**. General Procedure B: **20** (400 mg, 1.0 mmol), thionyl chloride (214  $\mu$ L, 2.75 mmol), *cis*-1,5-cyclooctanediol (728 mg, 5.0 mmol), and  $K_2CO_3$  (380 mg, 2.75 mmol) gave **70** as a yellow solid (342 mg, 65%); mp 69–72 °C; IR ( $cm^{-1}$ ) 3440, 2928, 2360, 1707, 1520;  $^1H$  NMR (300 MHz,  $CDCl_3$ )  $\delta$  1.29–1.83 (m, 12H, CH) 3.18–3.24 (m, 1H, OCH), 3.52–3.59 (m, 1H, HOCH), 4.20 (d, 1H,  $J = 15.3$  Hz,  $N-CH$ ), 4.86 (d, 1H,  $J = 15.3$  Hz,  $N-CH'$ ), 7.18–7.03 (m, 7 H, Ar–H), 7.60–7.52 (m, 2H, Ar–H), 7.95–7.91 (m, 3H, Ar–H and  $C(O)=C=CH$ );  $^{13}C$  NMR (75 MHz,  $CDCl_3$ )  $\delta$  20.1, 20.3, 33.9, 34.3, 35.9, 36.5, 42.8, 71.2, 73.6, 94.5, 123.1, 123.6, 124.1, 128.1, 128.3, 129.7, 130.2, 131.8, 132.6, 134.8, 137.6, 144.9, 145.9, 147.2, 168.4; CHN.

**3-(4-Chlorophenyl)-3-(3-hydroxy-2,2-dimethylpropoxy)-2-(4-nitrobenzyl)-2,3-dihydroisoindol-1-one (73)**. General Procedure B: **20** (400 mg, 1.0 mmol), thionyl chloride (214  $\mu$ L, 2.75 mmol), and neopentyl glycol  $K_2CO_3$  (526 mg, 5.0 mmol) gave **73** as an off-white solid (267 mg, 55%); mp 91–94 °C; IR ( $cm^{-1}$ ) 3425, 3077, 2959, 2871, 2160, 1689, 1606, 1519, 1468;  $^1H$  NMR (300 MHz,  $CDCl_3$ )  $\delta$  0.83 (d, 6H,  $J = 3.9$  Hz,  $(CH_3)_2$ ), 1.71 (br s, 1H, OH), 2.63 (d, 1H,  $J = 8.7$  Hz, OCH), 2.78 (d, 1H,  $J = 8.7$  Hz, OCH'), 3.37–3.42 (m, 2H,  $HOCH_2$ ), 4.44 (d,  $J = 15.3$  Hz, 1H,  $N-CH$ ), 4.58 (d,  $J = 15.3$  Hz, 1H,  $N-CH'$ ), 7.12–7.15 (m, 5 H, Ar–H), 7.28–7.32 (m, 2H, Ar–H), 7.55–7.58 (m, 2H, Ar–H), 7.93–7.96 (m, 1H,  $C(O)=C=CH$ ), 7.98–8.02 (m, 2H, Ar–H);  $^{13}C$  NMR (75 MHz,  $CDCl_3$ )  $\delta$  21.8, 36.4, 42.4, 69.0, 69.6, 94.5, 123.2, 123.2, 123.8, 127.9, 128.6, 129.9, 130.2, 131.6, 133.1, 134.9, 137.3, 144.6, 145.2, 147.3, 168.3; MS (ESI+)  $m/z$  481  $[M + H]^+$ . CHN.

**3-(4-Chlorophenyl)-3-(1-hydroxymethylcyclopropylmethoxy)-2-(4-nitrobenzyl)-2,3-dihydroisoindol-1-one (74)**. General Procedure B: **20** (400 mg, 1.0 mmol), thionyl chloride (214  $\mu$ L, 2.75 mmol), 1,1-bis(hydroxymethyl)cyclopropane (0.2 mL, 2.0 mmol), and  $K_2CO_3$  (526 mg, 5.0 mmol). Chromatography (Biotage SP4, silica; 10–50% EtOAc, petrol) gave **74** as a cream solid (442 mg, 92%); mp 148–149 °C. IR ( $cm^{-1}$ ) 3471, 3076, 2878, 1705, 1599, 1514  $cm^{-1}$ ;  $^1H$  NMR (300 MHz,  $CDCl_3$ ) 0.12–0.22 (m, 2H,  $CH_2$ ), 0.40–0.43 (m, 2H,  $CH_2$ ), 2.81 (s, 2H,  $OCH_2$ ), 3.43–3.51 (m, 2H,  $HOCH_2$ ), 4.49 (s, 2H,  $N-CH_2$ ), 7.12–7.19 (m, 5 H, Ar–H), 7.32–7.29 (m, 2H, Ar–H), 7.55–7.52 (m, 2H, Ar–H), 7.89–7.92 (m, 1H,  $C(O)=C=CH$ ), 7.98–8.01 (m, 2H, Ar–H);  $^{13}C$  NMR (75 MHz,  $CDCl_3$ ), 8.9, 8.9, 22.7, 42.8, 67.8, 95.0, 123.5, 123.6, 124.1, 128.3, 129.0, 130.2, 130.5, 131.9, 133.5, 135.3, 137.5, 144.9, 145.5, 168.5; HRMS ( $C_{26}H_{23}ClN_2O_5$ ) Calcd, 478.1290; obsd, 478.1291; CHN.

Separation of enantiomers was achieved by chiral preparative HPLC (Daicel Chiralpak AD-H 250  $\times$  10 mm; Hexane/Ethanol (4:1) 3.5 mL/min)

**(+)-R-3-(4-Chlorophenyl)-3-(1-hydroxymethylcyclopropylmethoxy)-2-(4-nitrobenzyl)-2,3-dihydroisoindol-1-one (74a)**.

Yellow solid,  $R_t = 16.5$  min. Optical rotation: specific rotation  $[\alpha]_D^{25} = +22.66^\circ$  (at 24.8 °C, wavelength = 589 nm, tube length = 0.25 dm, concentration = 0.406 g/100 mL).

**(-)-S-3-(4-Chlorophenyl)-3-(1-hydroxymethylcyclopropylmethoxy)-2-(4-nitrobenzyl)-2,3-dihydroisoindol-1-one (74b)**.

Off-white solid,  $R_t = 22.5$  min. Optical rotation: specific rotation

$[\alpha]_D^{25} = -20.10^\circ$  (at 24.8 °C, wavelength = 589 nm, tube length = 0.25 dm, concentration = 0.398 g/100 mL).

**3-(4-Chlorophenyl)-3-(4-hydroxycyclohexyloxy)-2-(4-nitrobenzyl)-2,3-dihydroisoindol-1-one (75)**. General Procedure B: **20** (400 mg, 1.0 mmol), thionyl chloride (214  $\mu$ L, 2.75 mmol), *cis/trans*-1,4-cyclohexanediol (586 mg, 5.0 mmol), and  $K_2CO_3$  (526 mg, 5.0 mmol) gave **75** as a white solid (338 mg, 68%); mp 88–91 °C; IR ( $cm^{-1}$ ) 3412, 3076, 2935, 2861, 2159, 1694, 1606, 1519, 1490, 1468, 1424;  $^1H$  NMR (300 MHz,  $CDCl_3$ ) mixture of diastereoisomers:  $\delta$  1.26–1.86 (m, 11H, OH and Cy-H), 3.09–3.26 (m, 1H, OCH), 3.62–3.70 (m, 1H,  $HOCH$ ), 4.78 and 4.24 (d: AB,  $J = 15.0$  Hz, 2H,  $N-CH_2$ ), 7.02–7.18 (m, 7H, Ar–H), 7.51–7.56 (m, 2H, Ar–H), 7.90–7.93 (m, 3H,  $O_2N-C-CH$  and  $C(O)=C=CH$ );  $^{13}C$  NMR (75 MHz,  $CDCl_3$ ) mixture of diastereoisomers  $\delta$  29.0, 29.2, 30.3, 30.7, 31.0, 32.3, 32.5, 42.7, 67.7, 68.6, 69.2, 71.4, 94.3, 94.3, 123.1, 123.8, 128.2, 128.2, 128.3, 128.3, 129.7, 130.2, 130.2, 131.6, 132.7, 134.7, 144.8, 146.0, 147.2, 168.3; MS (ESI+)  $m/z = 493 [M + H]^+$ ; CHN.

**3-(4-Chlorophenyl)-3-(4-hydroxycyclohex-2-enyloxy)-2-(4-nitrobenzyl)-2,3-dihydroisoindol-1-one (76)**. General Procedure B: **20** (400 mg, 1.01 mmol), thionyl chloride (214  $\mu$ L, 2.75 mmol) and *trans*-1,4-cyclohex-2-enediol (576 mg, 5.0 mmol),  $K_2CO_3$  (526 mg, 5.0 mmol) gave **76** as a white solid (263 mg, 53%); mp 81–83 °C; IR ( $cm^{-1}$ ) 3077, 2935, 2860, 2159, 2026, 1699, 1606, 1519, 1490, 1468, 1424;  $^1H$  NMR (300 MHz,  $CDCl_3$ ) mixture of diastereoisomers:  $\delta$  1.14–2.12 (m, 4H,  $CH_2$ ), 3.67–3.77 (m, 2H,  $(OCH-)_2$ ), 4.19–4.34 (m, 4H,  $(HOCH)_2$  and  $(N-CH_2)_2$ ), 4.80 (d, 1H,  $J = 15$  Hz,  $N-CH'$ ), 4.87 (d, 1H,  $J = 15$  Hz,  $N-CH'$ ), 5.28–5.40 (m, 2H,  $(CH)_2$ ), 5.69–5.83 (m, 2H,  $(CH)_2$ ), 7.03–7.14 (m, 8H, Ar–H), 7.17–7.23 (m, 6H, Ar–H), 7.55–7.61 (m, 4H, Ar–H), 7.9–7.99 (m, 3H, Ar–H and  $C(O)=C=CH$ );  $^{13}C$  NMR (75 MHz,  $CDCl_3$ ) mixture of diastereoisomers:  $\delta$  28.6, 30.5, 30.9, 43.1, 65.8, 65.9, 68.3, 68.4, 94.8, 94.9, 123.5, 123.5, 124.2, 124.3, 128.6, 128.6, 128.65, 128.67, 123.0, 130.1, 130.2, 130.6, 130.7, 131.9, 133.2, 134.1, 134.6, 135.2, 137.6, 137.7, 145.0, 146.1, 147.6, 145.1, 168.6; MS (ESI+)  $m/z = 491 [M + H]^+$ . CHN.

**Determination of Inhibition of the MDM2-p53 Interaction Using a Binding Assay (ELISA)**. Assays were carried out as described previously.<sup>21</sup>

**Cell-Based Assays. Western Blot Analysis for p53 Activation in Intact Cells.** Western blot analysis of p53, MDM2, p21<sup>WAF1</sup> and actin proteins in cells treated with the MDM2-p53 antagonists was carried out as described previously.<sup>21</sup> Detection of  $\alpha$ -tubulin on Western blots with the Clone DM1A monoclonal antibody (Sigma-Aldrich, Dorset, U.K.) at 1:2000 dilution was used as an additional protein loading control.

**Cellular Growth Inhibition ( $GI_{50}$ ).** The concentrations of compounds required for inhibition of cell growth by 50% ( $GI_{50}$ ) were determined for a range of cell lines of differing MDM2 and p53 gene status. The MDM2 amplified cell lines tested were SJSA-1 osteosarcoma, as well as LS and NGP neuroblastoma. The MDM2 nonamplified cell lines comprised SaOS-2 (p53 null osteosarcoma) and an isogenic matched pair of p53 wild-type and deleted colorectal carcinoma cell lines (HCT116 +/+ and HCT116 -/-). All cell cultures were grown in RPMI 1640 medium (Gibco, Paisley, U.K.) supplemented with 10% fetal calf serum and routinely tested and confirmed negative for mycoplasma infection. The growth of cells and their inhibition were measured using the sulphorhodamine B (SRB) method, as previously outlined.<sup>26,27</sup> Cells were seeded into 96-well tissue culture plates and incubated at 37 °C in a 5%  $CO_2$  humidified incubator for 24 h, after which the medium was replaced with 100  $\mu$ L of test medium containing a range of MDM2-p53 antagonist concentrations and incubated for a further 72 h to allow cell growth before adding 25  $\mu$ L of 50% trichloroacetic acid (TCA) to fix the cells for 1 h at 4 °C. The TCA was washed off with distilled water and 100  $\mu$ L of SRB dye (0.4% w/v in 1% acetic acid; Sigma-Aldrich, Poole, Dorset) was added to each well of the plate. Following incubation with the SRB dye at room temperature for 30 min, the plates were washed with 1% acetic acid and left to dry over-

night. The SRB stained protein, which is a measure of the number of cells in a well, was then resuspended in 100  $\mu\text{L}$  of 10 mM Tris-HCl (pH 10.5) and the absorbance at  $\lambda = 590$  nm was measured in each well using a Spectra Max Pro 400 plate reader. The  $\text{GI}_{50}$  was calculated by nonlinear regression analysis of the data using Prism v4.0 statistical software.

## ■ ASSOCIATED CONTENT

**S Supporting Information.** Additional experimental details for compounds not included in the main section and analytical data for all compounds and intermediates. X-ray structure tables. Table of combustion analysis data. Additional Western blot analysis for **6**, **7**, **47**, **50**, and **53–55**. Additional SRB growth inhibitory data for **74**, **74a**, and **74b**. This material is available free of charge via the Internet at <http://pubs.acs.org>.

## ■ AUTHOR INFORMATION

### Corresponding Author

\*Tel.: +44 191 222 6645 (I.R.H.); +44 191 246 4420 (J.L.). Fax: +44 191 8591 (I.R.H.); +44 191 4301 (J.L.). E-mail: [i.r.hardcastle@ncl.ac.uk](mailto:i.r.hardcastle@ncl.ac.uk) (I.R.H.); [john.lunec@ncl.ac.uk](mailto:john.lunec@ncl.ac.uk) (J.L.).

## ■ ACKNOWLEDGMENT

The authors thank Cancer Research UK and the Wellcome Trust for funding. Use of the EPSRC Mass Spectrometry Service at the University of Wales (Swansea) is gratefully acknowledged.

## ■ ABBREVIATIONS USED

ATM, ataxia telangiectasia mutated; Bcl-XL, B-cell lymphoma-extra large; CHK1 and 2, checkpoint kinase 1 and 2; DCM, dichloromethane; DIPEA, diisopropylethyl amine; DNA-PK, DNA-dependent protein kinase; mCPBA, *meta*-chloroperbenzoic acid; MDM2, murine double minute 2; SRB, sulforhodamine B; THF, tetrahydrofuran

## ■ REFERENCES

- (1) Vousden, K. H.; Lu, X. Live or let die: the cell's response to p53. *Nat. Rev. Cancer* **2002**, *2*, 594–604.
- (2) Lane, D. P. Cancer. p53, guardian of the genome. *Nature* **1992**, *358*, 15–16.
- (3) Juntila, M. R.; Evan, G. I. p53—A Jack of all trades but master of none. *Nat. Rev. Cancer* **2009**, *9*, 821–829.
- (4) Oliner, J. D.; Kinzler, K. W.; Meltzer, P. S.; George, D. L.; Vogelstein, B. Amplification of a gene encoding a P53-associated protein in human sarcomas. *Nature* **1992**, *358*, 80–83.
- (5) Toledo, F.; Wahl, G. M. Regulating the p53 pathway: in vitro hypotheses, in vivo veritas. *Nat. Rev. Cancer* **2006**, *6*, 909–923.
- (6) Momand, J.; Zambetti, G. P.; Olson, D. C.; George, D.; Levine, A. The *mdm-2* oncogene product forms a complex with p53 protein and inhibits p53-mediated transactivation. *Cell* **1992**, *69*, 1237–1245.
- (7) Fuchs, S. Y.; Adler, V.; Buschmann, T.; Wu, X. W.; Ronai, Z. Mdm2 association with p53 targets its ubiquitination. *Oncogene* **1998**, *17*, 2543–2547.
- (8) Haupt, Y.; Maya, R.; Kazan, A.; Oren, M. Mdm2 promotes the rapid degradation of p53. *Nature* **1997**, *387*, 296–299.
- (9) Kubbutat, M. H. G.; Jones, S. N.; Vousden, K. H. Regulation of p53 stability by Mdm2. *Nature* **1997**, *387*, 299–303.
- (10) Chene, P. Inhibiting the p53-MDM2 interaction: An important target for cancer therapy. *Nat. Rev. Cancer* **2003**, *3*, 102–109.
- (11) Fischer, P. Peptide, peptidomimetic, and small-molecule antagonists of the p53-HDM2 protein-protein interaction. *Int. J. Pept. Res. Ther.* **2006**, *12*, 3–19.

(12) Weber, L. Patented inhibitors of p53–Mdm2 interaction (2006–2008). *Expert Opin. Ther. Pat.* **2010**, *20*, 179–191.

(13) Vassilev, L. T.; Vu, B. T.; Graves, B.; Carvajal, D.; Podlaski, F.; Filipovic, Z.; Kong, N.; Kammlott, U.; Lukacs, C.; Klein, C.; Fotouhi, N.; Liu, E. A. In vivo activation of the p53 pathway by small-molecule antagonists of MDM2. *Science* **2004**, *303*, 844–848.

(14) Shangary, S.; Qin, D.; McEachern, D.; Liu, M.; Miller, R. S.; Qiu, S.; Nikolovska-Coleska, Z.; Ding, K.; Wang, G.; Chen, J.; Bernard, D.; Zhang, J.; Lu, Y.; Gu, Q.; Shah, R. B.; Pienta, K. J.; Ling, X.; Kang, S.; Guo, M.; Sun, Y.; Yang, D.; Wang, S. Temporal activation of p53 by a specific MDM2 inhibitor is selectively toxic to tumors and leads to complete tumor growth inhibition. *Proc. Natl. Acad. Sci. U.S.A.* **2008**, *105*, 3933–3938.

(15) Yu, S.; Qin, D.; Shangary, S.; Chen, J.; Wang, G.; Ding, K.; McEachern, D.; Qiu, S.; Nikolovska-Coleska, Z.; Miller, R.; Kang, S.; Yang, D.; Wang, S. Potent and orally active small-molecule inhibitors of the MDM2-p53 interaction. *J. Med. Chem.* **2009**, *52*, 7970–7973.

(16) Mohammad, R. M.; Wu, J.; Azmi, A. S.; Aboukameel, A.; Sosin, A.; Wu, S.; Yang, D. J.; Wang, S. M.; Al-Katib, A. M. An MDM2 antagonist (MI-319) restores p53 functions and increases the life span of orally treated follicular lymphoma bearing animals. *Mol. Cancer* **2009**, *8*, 115.

(17) Grasberger, B. L.; Lu, T. B.; Schubert, C.; Parks, D. J.; Carver, T. E.; Koblisch, H. K.; Cummings, M. D.; LaFrance, L. V.; Milkiewicz, K. L.; Calvo, R. R.; Maguire, D.; Lattanze, J.; Franks, C. F.; Zhao, S. Y.; Ramachandran, K.; Bylebyl, G. R.; Zhang, M.; Manthey, C. L.; Petrella, E. C.; Pantoliano, M. W.; Deckman, I. C.; Spurlino, J. C.; Maroney, A. C.; Tomczuk, B. E.; Molloy, C. J.; Bone, R. F. Discovery and cocrystal structure of benzodiazepinedione HDM2 antagonists that activate p53 in cells. *J. Med. Chem.* **2005**, *48*, 909–912.

(18) Koblisch, H. K.; Zhao, S. Y.; Franks, C. F.; Donatelli, R. R.; Tominovich, R. M.; LaFrance, L. V.; Leonard, K. A.; Gushue, J. M.; Parks, D. J.; Calvo, R. R.; Milkiewicz, K. L.; Marugan, J. J.; Raboisson, P.; Cummings, M. D.; Grasberger, B. L.; Johnson, D. L.; Lu, T. B.; Molloy, C. J.; Maroney, A. C. Benzodiazepinedione inhibitors of the Hdm2: p53 complex suppress human tumor cell proliferation in vitro and sensitize tumors to doxorubicin in vivo. *Mol. Cancer Ther.* **2006**, *5*, 160–169.

(19) Lu, Y.; Nikolovska-Coleska, Z.; Fang, X.; Gao, W.; Shangary, S.; Qiu, S.; Qin, D.; Wang, S. Discovery of a nanomolar inhibitor of the human murine double minute 2 (MDM2)-p53 interaction through an integrated, virtual database screening strategy. *J. Med. Chem.* **2006**, *49*, 3759–3762.

(20) Allen, J. G.; Bourbeau, M. P.; Wohlhieter, G. E.; Bartberger, M. D.; Michelsen, K.; Hungate, R.; Gadwood, R. C.; Gaston, R. D.; Evans, B.; Mann, L. W.; Matison, M. E.; Schneider, S.; Huang, X.; Yu, D.; Andrews, P. S.; Reichelt, A.; Long, A. M.; Yakowec, P.; Yang, E. Y.; Lee, T. A.; Oliner, J. D. Discovery and optimization of chromenotriazolopyrimidines as potent inhibitors of the mouse double minute 2-tumor protein 53 protein–protein interaction. *J. Med. Chem.* **2009**, *52*, 7044–7053.

(21) Hardcastle, I. R.; Ahmed, S. U.; Atkins, H.; Farnie, G.; Golding, B. T.; Griffin, R. J.; Guyenne, S.; Hutton, C.; Kallblad, P.; Kemp, S. J.; Kitching, M. S.; Newell, D. R.; Norbedo, S.; Northen, J. S.; Reid, R. J.; Saravanan, K.; Willems, H. M. G.; Lunec, J. Small-molecule inhibitors of the MDM2-p53 protein–protein interaction based on an isoindolinone scaffold. *J. Med. Chem.* **2006**, *49*, 6209–6221.

(22) Kitching, M. S.; Clegg, W.; Elsegood, M. R. J.; Griffin, R. J.; Golding, B. T. Synthesis of 3-alkoxy and 3-alkylamino-2-alkyl-3-arylisoindolinones. *Synlett* **1999**, 997–999.

(23) Naik, A. D.; Marchand-Brynaert, J.; Garcia, Y. A simplified approach to *N*- and *N,N*-linked 1,2,4-triazoles by transamination. *Synthesis* **2008**, *2008*, 149–154.

(24) Riedinger, C.; Endicott, J. A.; Kemp, S. J.; Smyth, L. A.; Watson, A.; Valeur, E.; Golding, B. T.; Griffin, R. J.; Hardcastle, I. R.; Noble, M. E.; McDonnell, J. M. Analysis of chemical shift changes reveals the binding modes of isoindolinone inhibitors of the MDM2-p53 interaction. *J. Am. Chem. Soc.* **2008**, *130*, 16038–16044.

(25) Park, C.-M.; Bruncko, M.; Adickes, J.; Bauch, J.; Ding, H.; Kunzer, A.; Marsh, K. C.; Nimmer, P.; Shoemaker, A. R.; Song, X.; Tahir,

S. K.; Tse, C.; Wang, X.; Wendt, M. D.; Yang, X.; Zhang, H.; Fesik, S. W.; Rosenberg, S. H.; Elmore, S. W. Discovery of an orally bioavailable small molecule inhibitor of prosurvival B-cell lymphoma 2 proteins. *J. Med. Chem.* **2008**, *51*, 6902–6915.

(26) Skehan, P.; Storeng, R.; Scudiero, D.; Monks, A.; McMahon, J.; Vistica, D.; Warren, J. T.; Bokesch, H.; Kenney, S.; Boyd, M. R. New colorimetric cytotoxicity assay for anticancer-drug screening. *J. Natl. Cancer Inst.* **1990**, *82*, 1107–1112.

(27) Nutt, J. E.; Lazarowicz, H. P.; Mellon, J. K.; Lunec, J. Gefitinib (“Iressa”, ZD1839) inhibits the growth response of bladder tumour cell lines to epidermal growth factor and induces TIMP2. *Br. J. Cancer* **2004**, *90*, 1679–1685.